Finite Element Modeling of the Fastening Systems and Concrete Sleepers in North America

Z. Chen[1], M. Shin[1], B.O. Andrawes[1]
[1]*University of Illinois at Urbana-Champaign, Urbana, IL, USA*

1. ABSTRACT:

Ensuring safety and serviceability of railways in North America has been an important issue due to increase in gross rail loads and cumulative freight tonnages on heavy haul railways as well as raising interest in higher-speed passenger rail development. Therefore, improving the performances of the fastening systems and the concrete sleepers according to the increased demand is in need. This study focuses on developing a 3D finite element (FE) modeling frame work of the fastening system and concrete sleeper to improve the knowledge regarding its mechanical behavior, and to provide reference for a new design guide-line. Model characteristics are first developed in the 2D model and then implemented in the 3D model. In this 3D FE model, following important mechanisms that are critical to the performance of fastening systems and concrete sleepers are included: 1) Frictional interaction between components of the fastening system, 2) Structural behavior of prestressed concrete sleepers, 3) Plastic behavior of each component in the system. The behaviors of each component, including the mechanical interactions, are validated with experimental tests. Good agreement is observed between the output of the 2D finite-element model and laboratory test data. Using the validated FE model, the system performances under different loading scenarios (vertical and lateral loading combinations) are compared. The results of current research work show FE modeling to be a useful tool and could be used in further investigation.

2. INTRODUCTION

With the development of high speed rail corridors and ever increasing axle loads in North America, there is an increasing demand on the railroad infrastructure and its components. Furthermore, the dominant design approach for the concrete sleeper and fastening system still remain mainly iterative. This is evident by the fact that the relation using speed and traffic to determine the design load in American Railroad Engineering and Maintenance-of-way Association (AREMA)'s Recommended Practices has been developed empirically [1]. To ensure that freight and passengers are transported safely and that proper track geometry is maintained, further investigation into the behavior and interaction of the concrete sleeper and fastening system is needed. In addition, a mechanistic design approach based on detailed structural analysis would be beneficial for infrastructure manufacturers to reduce costs on overdesigned parts and efficiently improve future design work.

Researchers have done some innovative studies in the modeling of the concrete sleepers and fastening systems. Yu and Jeong [2] presented a 3D finite element model including a prestressed concrete sleeper and ballast. Prestress and direct uniaxial, static railseat loading is applied to the model. A quarter-symmetric model was used to compare the performance of the concrete sleeper on different support conditions. The model is limited as it assumes full bond between the concrete and strand, hence it ignores the possibility of relative slip of strands causing the effect of prestress to be magnified. Yu et al. [3] presented an improved finite element model of the concrete sleeper with ballast and subgrade support. In this model the interaction between concrete and strand is modeled as cohesive element which is incorporated between them to simulate a linear force-slip relationship based on experimental data [4]. With the model built, several factors that could affect the performance of the concrete sleeper are investigated including strand pattern and different loading application. As the modeling of concrete sleeper and fastening system is a broad topic, various researchers have used finite element analysis to gain a better understanding about its behavior and their research work provided some insight into the application of this technique [5, 6].

Based on a thorough literature review some potential for improvement could be summarized and implemented in this research. As part of a large project funded by the Federal Railroad Administration (FRA) aimed at further understanding and improving the concrete sleeper and fastening system, the objective of this research is to build a detailed finite element model of the concrete sleeper and fastening system. The model will serve as a tool which will provide theoretical comparison for ongoing laboratory and field testing as well as a tool to perform parametric studies of component material properties and geometric dimensions. These studies would be conducted to serve the general goal of developing new mechanistic design criteria for the concrete sleeper and fastening system to satisfy the ever-increasing loading demands in North America. In this paper a detailed 3D concrete sleeper and fastening system model is presented under various loading scenarios including prestress force, vertical wheel loading and lateral wheel loading at different levels. The finite element program ABAQUS was utilized in the study. Nonlinear material properties are defined for components based on manufacturer data. Frictional interaction is defined between different components. A study is conducted using the model on how different lateral/vertical loading ratio would affect the load path through fastening system and the stress state of the system.

3. MODELING CONFIGURATION

3.1 SYSTEM DESCRIPTION

Fig. 1 illustrates the layout of the fastening system in the FE model. As shown, the fastening system is fixed to the concrete sleeper to transmit loading from the rail to the concrete surface and maintain uniform track geometry. Fastening systems of various designs are used in practice and different systems consist of different components. The fastening system modeled in this paper includes embedded iron shoulders, clips, nylon insulators, and a two part rail pad assembly consisting of a resilient polyurethane 95 Shore A pad for load attenuation and a nylon 6/6 abrasion plate to mitigate abrasion of the concrete. The embedded shoulder provides support for other components. The clip is deformed initially and inserted into shoulder to prevent longitudinal and lateral displacement of the rail. The insulator is placed between the clip and rail and between the rail base and shoulder to provide electrical isolation between the two rails to ensure the signal system is not shunted. In the working environment, the wheel loading can be divided into a vertical load, which is applied on the head of rail, and a lateral load that is pointing from the gage side to the field side. In this model the simplified geometries of all the components are used.

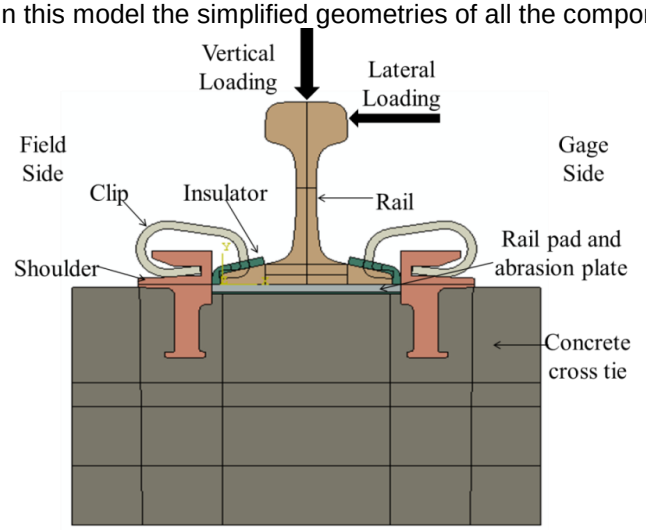

Fig. 1 Example layout of rail fastening system

3.2 CONSTITUTIVE RELATIONSHIPS

Concrete damaged plasticity model is used to define the concrete material property [7]. In this material model, two main failure mechanisms are considered, namely, tensile cracking and compressive crushing. Under uniaxial tension, concrete first goes through a linear-elastic stage,

and when stress reaches cracking stress it follows a softening stress-strain relationship. Under uniaxial compression the initial response is linear until the yielding stress is reached. In the plastic stage the response is first characterized by strain hardening and then strain softening after reaching its compressive ultimate stress. As cyclic loading is not included in the current model, two damage parameters related to unloading stiffness are not defined.

For all the fastening system components including shoulder, clip, rail pad, abrasion plate, insulator as well as the rail, a two-stage material property model is defined. In the beginning it follows an elastic relationship, and the plastic stage consists of a strain-hardening range followed by a strain-softening range. These components are modeled with 3D solid element.

3.3 COMPONENT INTERACTION

Interaction between different fastening system components is defined with contact pairs in ABAQUS [7]. A master surface and a slave surface of different mesh densities are identified.Some of the coefficient of friction (CoF) values were based on a series of large-scale abrasion resistance tests that were conducted recently at the University of Illinois at Urbana-Champaign (UIUC), but are not published yet, and others are from the literature review.To focus on the interaction between concrete and fastening system, the concrete sleeper is simplified into a concrete block that is close to the support of fastening system. Prestressed strands are not modeled and the effect of concrete prestress is considered through applying a predefined stress field in concrete that result in a uniform lateral compressive stress of 6.21 MPa. The value is determined after reviewing the effective prestress around shoulder in a full-scale concrete sleeper model.

The interaction between the concrete block and shoulder inserts is difficult to simulate as it is related to multiple surface and could have tensile stress between the two components. In this model the cohesive stress between concrete and shoulder inserts are ignored. Slots according to the geometry of shoulder inserts are cut in concrete and interaction pairs are defined between the internal surfaces of concrete and the surface of shoulder inserts, which means that only compressive interaction is considered in the model. Based on the manufacturer design, the gap between insulator and shoulder could not be explicitly determined as the position relationship is not described in detail. In 3D model the gap is set to be 0.127 mm, as in experiment relative sliding between concrete and abrasion plate was observed, but the support of shoulder prevents large relative displacement. This is important because the interaction between the shoulder and insulator considerably affects the load path through the fastening system under lateral loading. Due to this gap, lateral resistance first comes from the friction between the abrasion plate and concrete and the uneven clamping force due to rail sliding. As the insulator and shoulder come in contact, the resistance from the shoulder will share part of the loading.

3.4 BOUNDARY CONDITION AND LOADING

In the model boundary condition was applied at the lateral and bottom surface of concrete to provide lateral and vertical resistance for the system. The boundary condition was designed in this way to simulate laboratory test environment. In addition, temporary boundary conditions were applied to all the model components to stabilize the system and were later removed under loading.

Multiple analysis steps were defined to apply different types of loading. In the first step, prestress was applied on concrete with a predefined stress field and interactions were initiated with temporary loadings. In the second step, pressure loadings were applied on the toe surface of clips to simulate the process of clip lifting. A load of 15.6 kN was applied to exert excessive deformation prior to releasing the clip toe in following step. The pressure loading increased linearly with time. In the third step, the pressure on the toe of insulator gradually decreased with time as the clips were slowly released on to the insulator to apply the design clamping force. In the fourth step, a vertical load of 133 kN was introduced on the rail head, and in the fifth step, a lateral load was introduced according to the loading scenario. The loading combination was designed according to the loading environment expected to be encountered in North American

low-speed (speed lower than 64.4 km per hour) mainline freight segment. The distribution of loading between concrete sleepers at a spacing of 482.6 mm was assumed and the ratios between lateral and vertical (L/V) loading considered in the 3D model were 0.25, 0.375 and 0.5 [1]. Both of the loads were introduced as pressure over a small area to simulate the contact patch in practice.

4. MODEL VALIDATION

4.1 CONCRETE SLEEPER AND FASTENING SYSTEM IN 2D MODEL

The 2D mode of the concrete sleeper and fastening system was built and tested under a vertical load of 160.1 kN and clamping force of 22.2 kN. In order to ensure the credibility of the 2D model, the compression of the rail pad and the abrasion plate was compared with the analytically computed compression value of the pad and plate. The analytical compression value was calculated based on the assumption that the clamping force and vertical force were uniformly applied to the top of the rail pad, and it was found to be 0.158 mm while the average compression found from the model was 0.158 mm. Also, the force and deflection relationships of a clip model and a manufacture data were compared in Fig. 2. As shown in the figure, the behavior of the clip model strongly agreed with the manufacturer data.

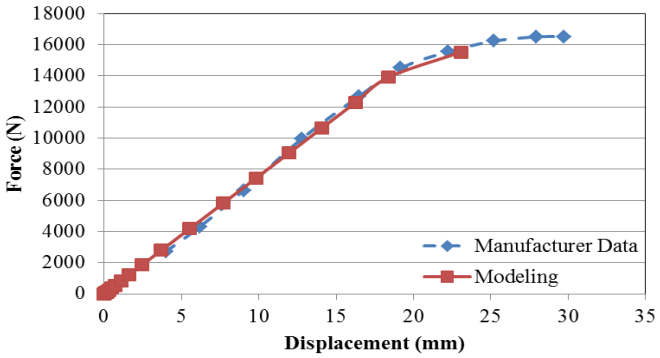

Fig.2. Comparisons of the force-displacement relationship of a clip model and a manufacturer data

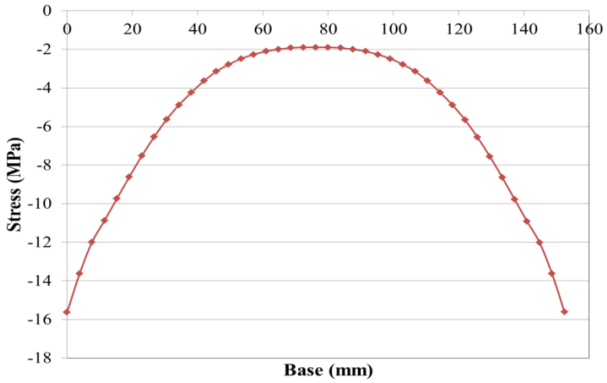

Fig. 3. Normal stress distribution on the top of the rail pad.

Fig. 3 shows the normal stress distribution on the top of the rail pad under the clamping force. The x axis represents the width of the rail pad underneath of the rail, while the y axis represents the compressive normal stress. This shows that the stress was higher at the edges of the pad than at the center of the pad due to the location of the clips of the fastening system. Also, the applied total clamping force transmitted into the rail pad was 22.4 kN. Therefore, it was confirmed that the clamping force was well transmitted from the clip, to insulator, to rail, and to the pad.

5. RESULTS

In working condition the wheel of a vehicle would apply both a vertical load and a lateral load to the rail through the contact patch on the top and lateral surface of rail head. On curved track, the loading condition can generally be characterized with the ratio between vertical and lateral load (L/V ratio). In this model three L/V ratios of 0.25, 0.375 and 0.5 were considered. After prestress and clamping forces were applied, a vertical load of 13.6 kN was applied on the top of rail head as pressure loading over an area of 645.16 mm^2. As the rail was relatively stiff it distributed the compressive stress onto a small area in the center of rail pad. Under vertical loading the dominant behavior of rail pad and abrasion plate was due to Poisson's effect as they expanded laterally. Friction resisted the lateral movement between the rail pad and abrasion plate as well as between abrasion plate and concrete-leading to an almost circular distribution. Afterwards a lateral loading according to the L/V ratio was applied on a small area at the lateral surface of rail head.

5.1 STRESS ANALYSIS

The maximum tensile and compressive stresses of different components under different loading scenarios are summarized in Table 1. As the stress distributions among the three L/V ratios are similar, only the cases with L/V ratios of 0.25 and 0.5 are listed to show the range of stress.

In concrete, compressive stress concentration was observed around the insert of shoulder. The stress concentration was due to the combination of the clamping force and lateral loading, and based on the stress contour the concrete is already crushed. In Fig. 4, it was observed that the compression zone under abrasion plate also shifted to the field side due to the rotation of rail. High tensile stress was observed between the two inserts of shoulder as a result of lateral loading, and concrete was already cracked. Due to geometric and confinement effects, the concrete was able to reach compressive stresses higher than the ultimate strength of concrete.

Table 1. Maximum tensile and compressive stress of components under different loading scenarios

Component	Maximum compressive Stress (MPa)		Yielding Strength or fc' (MPa)	Maximum Tensile Stress (MPa)		Yielding or cracking Strength (MPa)
	L/V = 0.25	L/V = 0.5		L/V = 0.25	L/V = 0.5	
Concrete	147	233	48	11	10	6
Clip	1272	148	1262	1160	165	1262
Insulator	131	121	64	74	101	64
Rail Pad	27	49	8	1	9	8
Abrasion Plate	26	46	64	2	9	64
Rail	170	277.5	1034	95	219	1034

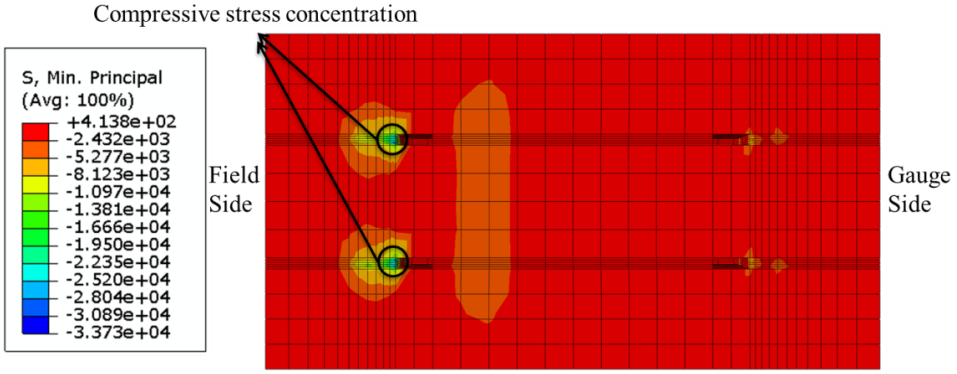

Fig.4. Concrete compressive stress contour in psi (L/V=0.5)

5.2 DEFLECTION ANALYSIS

The lateral resistance of rail consisted of several parts: the friction between rail and rail pad, the lateral component of clamping force and the support force transferred through the insulator when the gap between insulator and shoulder was closed. The displacements of rail head and rail base under vertical and lateral loading were important criteria as they determined the support condition of the wheel. The displacements of rail under vertical and lateral loading were a combination of translation and rotation: clamping force from clips acted as the resistance for rotation and friction between rail and rail pad acted as the resistance for translation.

Fig. 5 shows the relationship between the lateral load and the lateral displacements of the rail head and the rail base. For track alignment Federal Railroad Administration (FRA) Track Safety Compliance Manual [8] requires that on curved track of class 5 track the deviation of the mid-ordinate from a 9.4-meter chord may not be more than 12.7 mm. It was observed that the lateral displacement of rail head was smaller than 12.7 mm until lateral loading reached 57.8 kN. As the material of field-side insulator had already yielded, the lateral displacement of rail head increased more rapidly afterwards. The modeling result justified the field practice of using stiffer insulator on the field side. It is also required that the base of rail does not move laterally more than 12.7 mm relative to the crosstie, and the output of the model was within the acceptable range. As the gap between the insulator and the shoulder in the model was relatively small, it was soon closed right after the application of lateral loading. As a result, the shoulder prevented any further sliding of the rail and therefore the dominant mode of displacement was rotation. And any further lateral displacement of the rail base was due to the deformation of the insulator post and/or shoulder.

In this model the lateral bending stiffness of rail was ignored as the support condition on the ends of a rail segment was not simulated. In addition, the location of lateral loading was higher than that in the laboratory setting, which increased the arm of lateral loading and magnified the rotation of the rail. With these limitations the lateral displacement of rail was overestimated in this model.

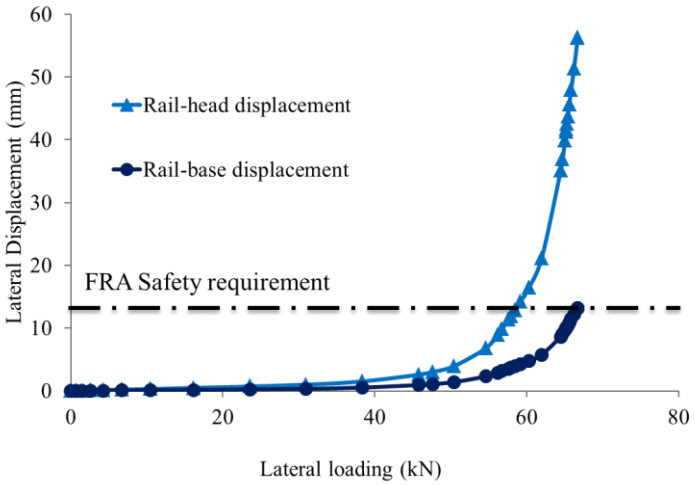

Fig.5. Relationship between lateral loading and rail lateral displacement

6. CONCLUSIONS

In this paper a detailed 2D and 3D finite element model for a sleeper and fastening system was presented. The FE model consisted of concrete sleeper and fastening system based on actual product design, and was loaded through practical static loadings after prestress was applied. Inelastic material properties as well as component tangential and vertical interactions were incorporated into the model. The FE Model was validated with the manufacturer data and analytical solutions. After the validation, the 3D FE model

was simulated with the different loading scenarios. Three loading scenarios were considered in the analysis (L/V=0.25, 0.375, 0.5). Some conclusions were summarized based on modeling output:

- Compressive stress concentration was observed around shoulder insert and resulted in concrete crushing. At the same time tensile stress concentration was observed between the two inserts of the shoulder leading to concrete cracking.
- Under L/V ratio of 0.5, yielding of the components was observed in the shoulder, the clip, the insulator, and the rail pad.
- The lateral displacement of the rail head satisfied the FRA safety requirement until lateral loading reached to 57.8 kN. Severe yielding was observed on the field-side insulator while deformation in the gauge-side insulator was smaller. The dominant displacement mode of the rail was rotation, and the lateral displacement of the rail-base was within the acceptable range even under a L/V load ratio of 0.5.

7. ACKNOWLEDGEMENT

The authors would like to express our sincere gratitude to the United States Department of Transportation (US DOT) Federal Railroad Administration (FRA) for providing funding for this research project. The published material in this paper represents the position of the authors and not necessarily that of the DOT. In addition, the authors want to thank Jose Mediavilla (Amsted RPS), Pelle Duong (CXT Concrete Ties), and the following FRA Sleeper and Fastener BAA Industry Partners for providing product information and advice for research work:

- Amsted RPS / Amsted Rail, Inc.
- BNSF Railway
- CXT Concrete Ties, Inc., LB Foster Company
- GIC Ingeniería y Construcción
- Hanson Professional Services, Inc.
- National Railway Passenger Corporation (Amtrak)
- Union Pacific Railroad

The authors also would like to specially thank Riley Edwards, Marcus Dersch, Professor Daniel Kuchma, Professor Erol Tutumluer and Professor David Lange for their invaluable insight and experience. This work would not be possible without the contribution from Christopher Rapp, Brandon Van Dyk, Ryan Kernes, Sihang Wei, Justin Grasse, and Amogh Shurpali.

8. REFERENCE

[1] American Railway Engineering and Maintenance-of-way Association (AREMA), AREMA manual Chapter 30 Ties, 2009.

[2] H. Yu, D.Y. Jeong, Finite Element Modeling of Railroad Concrete Sleeper – A Preliminary Study. International Conference of Railway Engineering (2010), Beijing, China.

[3] H. Yu, D.Y. Jeong, , J. Choros, and T. Sussmann, Finite Element Modeling of Prestressed Concrete Sleepers with Ballast and Subgrade Support, Proceedings of the ASME 2011 International Design Engineering Technical Conference & Computers and Information in Engineering Conference, DETC2011-47452., Washington, DC, USA. August 2011

[4] H. Abrishami, and D. Mitchell,Bond characteristics of pretensioned strand, ACI Materials Journal, 90(3), May-Jun. (1993) 228-235.

[5] A. Lundqvist, and T. Dahlberg, Load Impact on Railway Track due to Unsupported sleepers, Proc. IMechE Part F: J. Rail and Rapid Transit, 219, Part. F, (2005) 67-77.

[6] S. Kaewunruen, and A.M. Remannikov, Investigation of Free Vibrations of voided Concrete Sleepers in Railway Track System, Proc. IMechE Part F: J. Rail and Rapid Transit, 221, (2007) 495-507.

[7] Dassault Systèmes Simulia Corp. “ABAQUS Analysis User’s Manual.”

[8] Federal Railroad Administration. Track Safety Standards Compliance Manual: Chapter 5 Track Safety Standards Classes 1 through 5, 2006.